Ionics (2023) 29:2341–2349
https://doi.org/10.1007/s11581-023-04968-2

ORIGINAL PAPER

# Solid polymer electrolyte based on PEO/PVDF/$Mg(ClO_4)_2$-[EMIM][$ESO_4$] system for rechargeable magnesium ion batteries

Jesús Guzmán-Torres[1] · Edgar González-Juárez[1] · María de la Luz Hernández-Nieto[1] · Arián Espinosa-Roa[2] · Eduardo M. Sánchez[1]

Received: 16 December 2022 / Revised: 9 March 2023 / Accepted: 15 March 2023 / Published online: 5 April 2023


## Abstract

Solid polymer electrolyte (SPE) membranes were prepared using the solution-cast technique by mixing polyethylene oxide/polyvinylidene fluoride/magnesium perchlorate (PEO/PVDF/$Mg(ClO_4)_2$) ternary system with concentrations of 10, 20, 30, and 40 wt. % of the ionic liquid (IL) 1-ethyl-3-methylimidazolium ethyl sulfate [EMIM][$ESO_4$]. The SPE membrane of SPE:IL (60:40 wt. %) demonstrated several electrochemical properties that satisfy a potential application in rechargeable magnesium ion batteries (MIBs) such as good conductivity at room temperature (~$5.4 \times 10^{-5}$ S $cm^{-1}$) and high $Mg^{2+}$ ion transport number ($t_{Mg^{2+}} \sim 0.34$). The results by X-ray diffraction (XRD) revealed an amorphous structure, which favored the diffusion of $Mg^{2+}$ ions within the SPE structure. In addition, differential thermal analysis (DTA) showed the melting point at ~ 329 K. Fourier transform infrared spectroscopy (FTIR) confirmed the presence of characteristic functional groups in SPE membrane, identified by the appearance of the absorption bands C–O–C, $CH_2$, C–O, $ClO_4^-$, and C–O–S–O. The electrochemical stability window of ~ 4.2 V was determined using linear sweep voltammetry (LSV).

**Keywords** Solid polymer electrolyte (SPE) · Ionic liquid (IL) · Rechargeable magnesium ion batteries (MIBs)

## Introduction

Magnesium-based solid polymer electrolyte (SPE) membranes have been studied for their potential application in magnesium solid state batteries [1]. A wide variety of magnesium salts were used, for example, $MgCl_2$ [2], $Mg(NO_3)_2$ [3], $Mg(CH_3COO)_2$ [4], $MgSO_4$ [5], $Mg(ClO_4)_2$ [6], $Mg(CF_3SO_3)_2$ or $Mg(Tf)_2$ [7], and $Mg(N(CF_3SO_2)_2)_2$ or $Mg(TFSI)_2$ [6], dissolved in various polymeric systems, such as polyethylene oxide (PEO) [2], polyvinyl acetate (PVA) [3], polyvinyl pyrrolidone (PVP) [5], polyethylene carbonate (PEC) [6], polyethylene glycol (PEG) [4], and polyallyl glycidyl ether (PAGE) [8]. Likewise, there are several reports on SPE membranes prepared with copolymers and polymer blends as poly(ε-caprolactone-co-trimethylene carbonate) PCL-PTMC [9], biopolymers [10], the mixtures PEO-PVDF [11], and PEO-PVP [12].

The SPE membranes have low conductivities, therefore, is necessary to carry out various strategies to increase the ion mobility. Among the most used is gelation with solvents such as glymes (mono-, di-, tri-, and tetra-) [13] and carbonate esters (ethylene-, propylene-, or diethylene-) [14]. On the other hand, the plasticizers succinonitrile ($(NCCH_2)_2$) [15] and recently urea ($(NH_2)_2CO$) [16] were studied as additives to polymer magnesium salt system. A different approach for nanoparticles (MgO, $TiO_2$, $Al_2O_3$, $SiO_2$, and $B_2O_3$) as ionic conductivity changing agents in SPE membranes showed promising results [17].

The PEO is the most studied polymer [2], but its electrochemical and mechanical properties are poor. However, if a second polymer as polyvinylidene fluoride (PVDF) [11] or PVP [12] is added, these properties are enhanced. Dhatarwal and Sengwa [18] reported a decrease in the intensity of the X-ray peaks as the PVDF content in the polymer mixture increases. Considering the effect of incorporation PVDF into PEO, it is desirable to have a larger amount of PEO in the mixture since the oxygens in the PEO chains are responsible

✉ Eduardo M. Sánchez
eduardo.sanchezcv@uanl.edu.mx

1 Facultad de Ciencias Químicas, Universidad Autónoma de Nuevo León, Av. Universidad S/N Ciudad Universitaria, San Nicolás de los Garza, C.P. 66451 Nuevo León, Mexico

2 CONACyT–Centro de Investigación en Química Aplicada, Sur 204 Parque de Innovación E Investigación Tecnológica, Av. Alianza, 66629 Apodaca, Nuevo León, Mexico

for cation solvation. Otherwise, a problem may arise because PVDF is immiscible in small amounts in PEO [19]. Broadly, the mechanical and electrochemical performance of SPE membranes prepared using PVDF as an additive can be improved [20]. It was observed in the literature [21] that adding 10 wt. % of PVDF to PEO and combined it with an electrolytic salt of either lithium, sodium, or magnesium provides a solid polymeric structure suitable for preparing SPE membranes with acceptable ionic conductivity.

In the last years, ionic liquids (ILs) have been used as plasticizing or gelling agents to increase conductivity in SPE membranes. Maheshwaran et al. [22] published a study on the effect of 1-ethyl-3-methyl imidazolium tetrafluoroborate [EMIM][$BF_4$] incorporation within PEO/$Mg(CF_3SO_3)_2$ system, reporting a marked increase of ionic conductivity and $Mg^{2+}$ ion transport number ~ 0.22. Tang et al. [23] elaborated an electrolytic system formed by the copolymer polyvinylidene fluoride-co-hexafluoropropylene PVDF-HFP and the salt $Mg(CF_3SO_3)_2$ modified by the ionic liquid 1-ethyl-3-methyl imidazolium trifluoromethane sulfonate [EMIM][$CF_3SO_3$], which decreased the crystallinity in PVDF-HFP and increased the conductivity of SPE membranes. Rathika et al. [11] prepared solid polymer blend electrolytes by optimized blend of PVA-$Mg(CF_3SO_3)_2$-[EMIM][$CF_3SO_3$] system and the maximum ionic conductivity obtained at room temperature was $1.2\times10^{-5}$ S $cm^{-1}$ with the blend containing 15 wt. % salt.

While ILs are relatively expensive, Gupta et al. [24] presented a relatively cheap alternative variant using the ethyl sulfate anion ($SO_4CH_2CH_3$- or ES-), which displayed an electrochemical window of nearly 4 V in glassy carbon electrodes. Also, the magnesium ion is electrochemically active with polyaniline/platinum cathodes when dissolved in the ionic liquid 1-ethyl-3-methylimidazolium ethyl sulfate [EMIM][$ESO_4$] [25]. Therefore, ionic liquid [EMIM][$ESO_4$] is a viable candidate as an additive in SPE membranes that uses magnesium salt due to their excellent properties, such as high thermal stability, high ionic conductivity, low viscosity, wide electrochemical stability window, and protic nature [26–29].

The type and percentage of magnesium salt are important for possible technological application in the future. Salts with anions $[CF_3SO_3]^-$ and $[N(CF_3SO_2)_2]^-$ exhibit remarkable properties but at an unaffordable cost. Other anions such as $NO_3^-$ and $SO_4^{2-}$ show a smaller electrochemical window, lower conductivities, and are therefore not entirely desirable. Contrarily, the $ClO_4^-$ anion has a wide electrochemical window and consequently the $Mg(ClO_4)_2$ salt has been tested in polyelectrolyte systems [6].

To the best of our knowledge, there exists no previous experimental work describing the development of SPE membranes based on PEO/PVDF/$Mg(ClO_4)_2$-[EMIM][$ESO_4$] system. Hence, the purpose of this work is to prepare SPE membranes in which the $Mg(ClO_4)_2$ salt was selected as $Mg^{2+}$ ions supplier, to understand the effect of adding ionic liquid [EMIM][$ESO_4$] within the SPE-based electrolyte, evaluating their electrochemical performance in magnesium battery application.

## Experimental section

Polyethylene oxide (PEO, Sigma Aldrich Mv ~ 900,000), polyvinylidene fluoride (PVDF, Sigma Aldrich Mw ~ 534,000), 1-ethyl-3-methylimidazolium ethyl sulfate ([EMIM] [$ESO_4$], Sigma Aldrich, purity ≥ 95 %), and magnesium perchlorate ($Mg(ClO_4)_2$, Sigma Aldrich ACS reagent) were used to prepare SPE membranes. Acetone (ACE, Sigma Aldrich ACS reagent, purity ≥ 99.5 %) and dimethylacetamide (DMAc, Sigma Aldrich ReagentPlus, purity ≥ 99 %) were used as solvents in a 70:30 vol. % ratio, respectively. Stoichiometric amounts of PEO:PVDF (90:10 wt. %), $Mg(ClO_4)_2$, and [EMIM][$ESO_4$] were added to a glass vial in 5 ml solvent mixture; this mixture was sonicated for 12 h at 40 °C. Subsequently, the viscous mixture was cast over Teflon dishes and solvents were evaporated to obtain free-standing SPE membranes with a thickness from 200 to 300 µm. The SPE membranes were dried at 50 °C on a heating plate and then under vacuum to be stored in a dry box with an argon atmosphere. Table 1 lists all the mixtures prepared with the materials. The concentration of IL, magnesium salt, and polymers in SPE membranes was determined by the molar ratio of $CH_2$–O–$CH_2$ (EO)/$Mg^{2+}$/IL.

### Structural characterization

The structural characterization of the materials was analyzed by X-ray diffraction (XRD, D2 Phaser, Bruker) and Fourier transform infrared spectroscopy (FTIR, Interspec 200-X). The thermal stability was evaluated by differential thermal analysis (DTA-50, Shimadzu), and the semicrystalline nature of the SPE membranes was evidence with optical microscopy studies (MV-439, National Instruments).

### Coin cell assembly

CR2032 coin cells, made of SS316 for its excellent properties [30], were assembled with two configurations: SS||SPE||SS and Mg||SPE||Mg, to determine the total ion transport number and the $Mg^{2+}$ ion transport number, respectively. The impedance of the Mg||SPE||Mg cell was measured immediately before and after polarization. Electrochemical impedance spectroscopy (EIS) was evaluated in the frequency range of 1 Hz to 1 MHz by applying 10 mV amplitude signal. The cyclic voltammetry (CV) and linear sweep voltammetry (LSV) studies were performed using a

**Table 1** Raw material properties and SPE membranes showing the percentage of crystallization

| Sample | % Crystallization by XRD | Amorphous-semicrystalline transition of PEO Tt/°C | $AH_t$ (J/g) | % Relative crystallization of PEO by DTA |
|---|---|---|---|---|
| PEO | 53.0 | 67.4 | 172.1 | 100 |
| PEO:PVDF (90:10 wt. %) | 23.3 | 65.0 | 85.8 | 49.8 |
| SPE:IL (100:0 wt. %) | 20.8 | 58.6 | 20.7 | 12.0 |
| SPE:IL (90:10 wt. %) | 21.1 | 58.0 | 16.1 | 9.4 |
| SPE:IL (80:20 wt. %) | 15.5 | 59.2 | 19.5 | 11.3 |
| SPE:IL (70:30 wt. %) | 21.4 | 57.2 | 24.2 | 14.0 |
| SPE:IL (60:40 wt. %) | 21.9 | 56.4 | 60.2 | 35.0 |
| PVDF | 31.0 | NA | NA | NA |
| $MgClO_4$ | 57.2 | NA | NA | NA |

VMP3 potentiostat/galvanostat (Biologic Science Instruments) at scan rate of 5 mV $s^{-1}$. All cells were assembled in a dry glove box (Omni-Lab 0210, VAC) filled with argon and $H_2O < 1$ ppm.

## Results and discussion

### X-ray diffraction studies

Figure 1a displays the XRD pattern of raw materials, while Fig. 1b shows the XRD pattern of the SPE membranes compared to the base membrane 16 $Mg(ClO_4)_2$–84(PEO:PVDF (90:10 wt. %)) or SPE:IL (100:0 wt. %).

Based on Fig. 1a, PEO presents a maximum peak intensity at 23.6°, along with a second intense peak at 19.5°. Two lower intensity peaks can be observed at 26.6° and 27.2°, corresponding to diffractions from (112), (120), (131), and (041) planes, respectively, according to ICDD crystallographic file 00–057-1528. PVDF exhibits two main peaks at 18.5° and 20.0° and another minor peak at 26.7°, corresponding to crystallographic planes (110), (020), and (021), respectively, according to crystallographic file JCPDS No. 44–0141 [31]. The $Mg(ClO_4)_2$ shows three main peaks at 21.5°, 23.0°, and 31.6° corresponding to (021), (121), and (221) planes, respectively, according to JCPDS crystallographic file No. 85–0609 [32].

From Fig. 1b, the diffractogram of the SPE membrane with a composition PEO:PVDF (90:10 wt. %) exhibits a clear decrease in the intensity counts of the main peaks (5 times relative to PEO) located at 23.0° and 18.8°. Moreover, the disappearance of the main peaks associated with PVDF (18.5° and 20.0°) was observed, indicating that the polymeric chain of PVDF can plasticize PEO and significantly reduce its degree of crystallinity, which is helpful for the transport of $Mg^{2+}$ ions [12]. In addition, other minor peaks

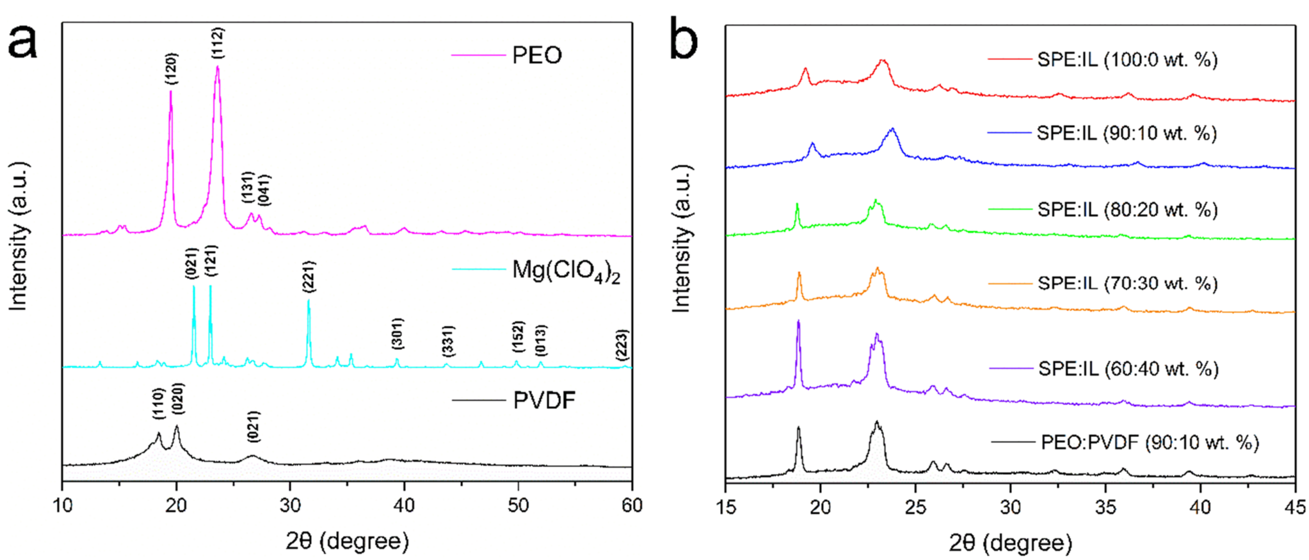


**Fig. 1** XRD pattern of **a** PEO, $Mg(ClO_4)_2$, PVDF, and **b** SPE membranes

were found in the diffractogram of the SPE membrane with composition PEO:PVDF (90:10 wt. %) located at 26.2°, 27.0°, 33.3°, 36.1°, and 39.6°, associated with PEO.

In the SPE membrane SPE:IL (100:0 wt. %), the (021) and (221) planes of $Mg(ClO_4)_2$ were not observed, possibly due to its efficient incorporation into the PEO-PVDF (90:10 wt. %) system. As a result of this incorporation, there is a decrease in crystallinity as well as a reduction in peak intensity counts from 3000 to 1500, which contributes to the ionic conductivity of the SPE membranes [33].

The $Mg(ClO_4)_2$ and [EMIM][$ESO_4$] incorporation into SPE membranes produce an increase in the 10° to 40° "hump," showing a decrease in crystalline nature of PEO, previously mentioned by number of counts, with a 10 wt. % PVDF addition. To quantify these observations, a formal analysis [34] using the percentage of crystallinity ($X_c$) was carried out using the area of crystalline peaks ($A_C$) and the combined area of crystalline and amorphous peaks (without "hump") and diffractogram total area ($A_T$), from 10 to 40°.

$$X_c = \left(\frac{A_C}{A_T}\right) \cdot 100 \quad (1)$$

Table 1 shows the crystallization percentage results (calculated by Origin Pro) for diffractograms shown in Fig. 1. These observations confirm a considerable decrease from 53 to 23 % in degree of crystallization when only 10 wt. % of PVDF was added to PEO network.

The percentage of crystallinity gradually decreased with the addition of $Mg(ClO_4)_2$ in the SPE membranes. However, the crystallinity did not decrease with the incorporation of the ionic liquid, except in the case of the SPE membrane SPE:IL (80:20 wt. %), indicating a stronger plasticizing effect with a small proportion of PVDF in the mixture.

A shift toward lower Bragg angles was likewise observed with the addition of IL at concentrations above 20 wt. %, indicating an effective interaction between IL and the PEO semicrystalline interlaminar layers, which increases the interlaminar spacing value. Besides, an increase in crystallite size was observed, as evidenced by interlaminar spacing measurements, SEM studies, Fig. S1, and Table S1 in the supplementary information.

## FTIR studies

Figure 2 displays FTIR spectra of starting materials (Fig. 2a) and the prepared SPE membranes (Fig. 2b). The spectra of PEO and PVDF were consistent with the FTIR spectra, published elsewhere [18]; the spectrum of $Mg(ClO_4)_2$ is coincident with FTIR spectra reported by Reddy and Chu [35]; and the spectrum of IL [EMIM][$ESO_4$] was similar to FTIR spectra reported by Nkuna et al. [36]. The SPE membrane formed by the incorporation of PVDF to the PEO matrix (10:90 wt. %, respectively) generally displays typical PEO bands, such as C–O stretching at 833 $cm^{-1}$ and $CH_2$ asymmetric bending at 952 $cm^{-1}$. Triplet splittings formed by symmetric and asymmetric stretching of C–O–C band were observed at 1055, 1100, and 1150 $cm^{-1}$ due to the effect of crystallinity decrease in PEO by PVDF addition. The vibrational bands observed in the wavenumbers 1240 and 1280 $cm^{-1}$, corresponding to $CH_2$ symmetric and asymmetric torsions, the doublet at 1345 and 1355 $cm^{-1}$, as well as 1471 $cm^{-1}$, were assigned to $CH_2$ bending. For relatively low percentage of PVDF in the base membrane (10 wt. %), fewer characteristic signals were observed for this compound, which were located at 875 $cm^{-1}$, corresponding to $CH_2$ stretching of PVDF, and possibly band at 750 $cm^{-1}$ with assignment to $CF_2$ bending

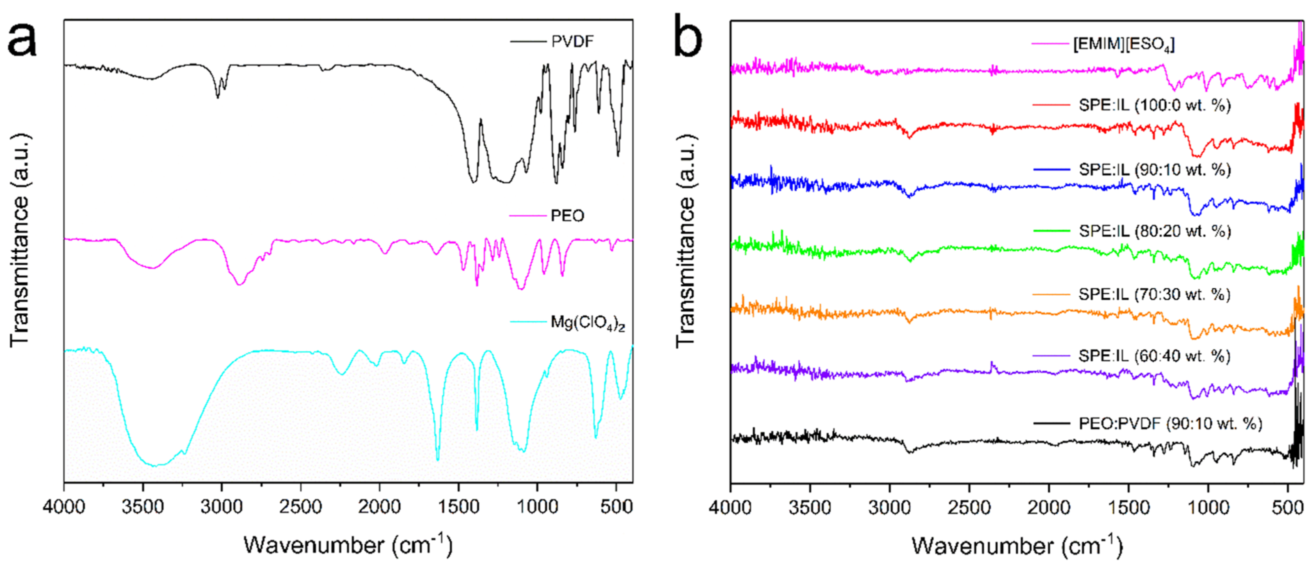


**Fig. 2** FTIR spectrum of **a** PEO, $Mg(ClO_4)_2$, PVDF, and **b** SPE membranes

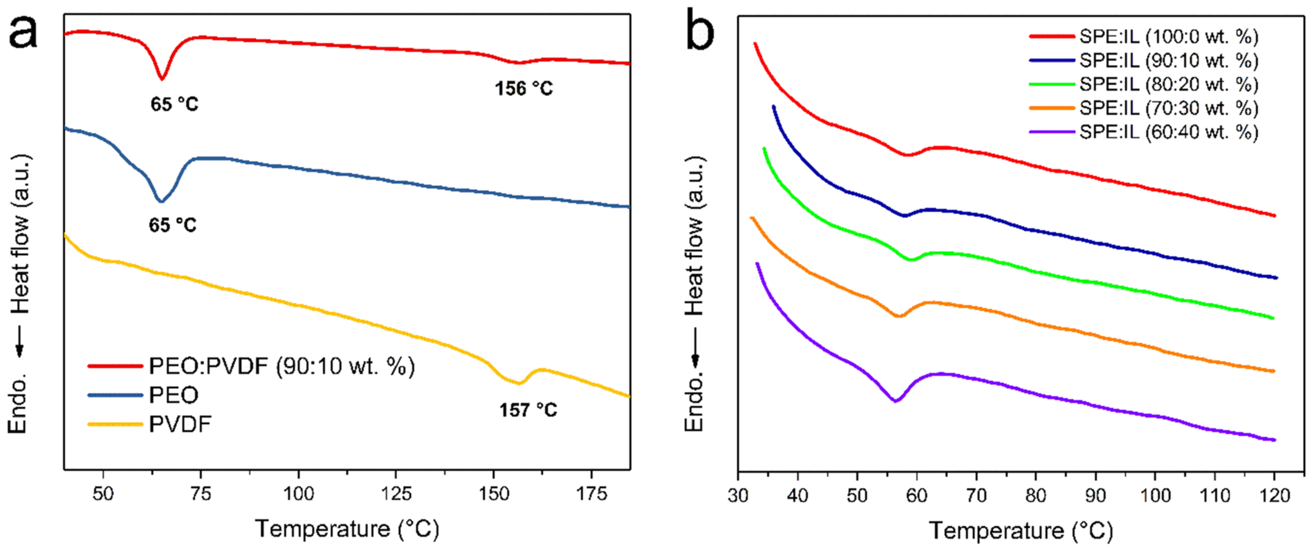


**Fig. 3** DTA curves of **a** PEO:PVDF (90:10 wt. %), PEO, PVDF, and **b** SPE membranes

(both signals assigned to the PVDF α phase). The addition of $Mg(ClO_4)_2$ to PEO:PVDF (90:10 wt. %) system with a 16 wt. % to form a SPE membrane shows some characteristic weak bands, such as $ClO_4^-$ asymmetric bending at 624 $cm^{-1}$ and 1405 $cm^{-1}$, and a small band corresponding to $ClO_4^-$ symmetric stretching [37]. On the other hand, the strong vibration of $Mg(ClO_4)_2$ at 1642 $cm^{-1}$ disappears completely in all SPE membranes. These observations suggest the possible interaction of the $Mg^{2+}$ ions of salt with ether oxygen of PEO [22]. The absorption bands at 755, 905, 1015, 1175, 1210, and 1570 $cm^{-1}$ were assigned to C–O–S–O bending, C–O–$SO_3$ system, C–O–$SO_3$ symmetric stretching, an imidazolium ring asymmetric stretching in-plane, C–O–$SO_3$ asymmetric stretching, and C = N stretching, respectively [38]. In particular, it was observed an increase in the band at 1015 $cm^{-1}$, as well as decrease in the band at 1150 $cm^{-1}$, as the ionic liquid in the base membrane increases, which suggests possible interactions of $[EMIM]^+$ cation with the oxygens in the PEO polymeric chain [39].

## Thermal studies

Figure 3 shows a DTA analysis performed in SPE membranes. PVDF showed a melting temperature ($T_m$) at 157 °C and PEO at 65 °C; similarly, the SPE membrane PEO:PVDF (90:10 wt. %) showed both $T_m$ (Fig. 3a). The PEO thermogram evidenced a typical semi-crystalline to crystalline transformation process at 67.4 °C (see Table 1). The addition of PVDF indicates a slight reduction in the transition temperature to 65 °C as a function of the highest percentage (90 wt. %) was constituted by PEO. The addition of $Mg(ClO_4)_2$ to PEO:PVDF (90:10 wt. %) system produces a slight increase in the transition at 58.6 °C and the addition of 10 wt. % ionic liquid produces a decrease with a transition temperature at 58.0 °C, which increases with the increment of up to 20 % of [EMIM][$ESO_4$] with a value of 59.2 °C. Therefore, a higher ionic liquid addition produces reductions at the melting points, as seen in Fig. 3b. On the other hand, both the transition enthalpy and the relative percentage of crystallization (% $X_{C,el} = 100(\Delta H_{t,membrana})/(\Delta H_{t,PEO})$) show a decrease due to the PVDF addition (50 %, see Table 1). Additionally, both are reduced with the addition of 12 wt. % $Mg(ClO_4)_2$. These results, added to XRD analysis, where a decrease in crystallinity with the addition of ionic liquid from 10 wt. % to 20 wt. %, and an increase in crystallinity percentage with the

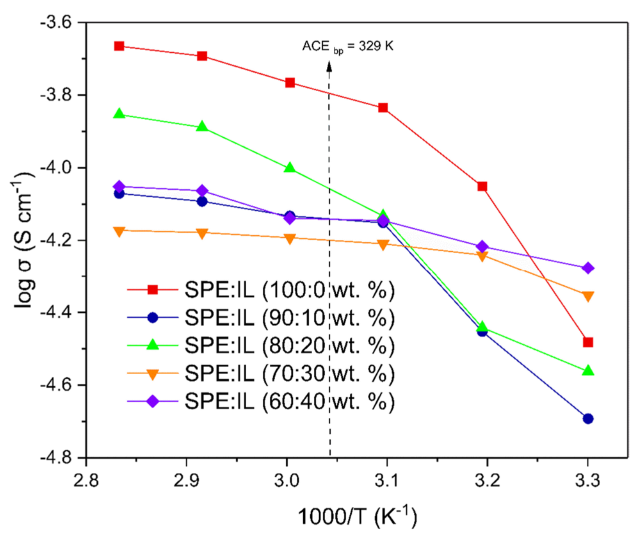


**Fig. 4** Arrhenius plot of temperature dependence ionic conductivity in SPE membranes. Lines are just guides to the eye. ACE boiling point is 329 K

**Table 2** Electrical properties of SPE membranes

| SPE membranes | Log($s_{RT}$/(S cm$^{-1}$) | $E_a^{RT}$/meV | Log($s_{T=80\,°C}$/(S cm$^{-1}$) | $E_a^{T=80°C}$/meV |
|---|---|---|---|---|
| SPE:IL (100:0 wt. %) | −5.08 | 351.4 | −4.43 | 51.1 |
| SPE:IL (90:10 wt. %) | −4.69 | 195.7 | −4.15 | 31.5 |
| SPE:IL (80:20 wt. %) | −4.56 | 98.4 | −4.13 | 36.7 |
| SPE:IL (70:30 wt. %) | −4.35 | 91.5 | −4.21 | 10.2 |
| SPE:IL (60:40 wt. %) | −4.27 | 48.4 | −4.15 | 12.0 |

addition of [EMIM][$ESO_4$]. This suggests that the addition of ionic liquid has a significant impact on the crystallinity of the mixture [40]. The largest reduction in crystallinity was produced by the combined addition of 10 wt. % PVDF to PEO and 16 wt. % $Mg(ClO_4)_2$, and moderate increases in crystallinity were achieved with the addition of ionic species such as $Mg^{2+}$, $[ClO_4]^-$, $[EMIM]^+$, and $[ESO_4]^-$ (see Figs. S2, S3, and S4 in the supplementary information for optical microscopy studies and density functional theory (DFT) studies, respectively).

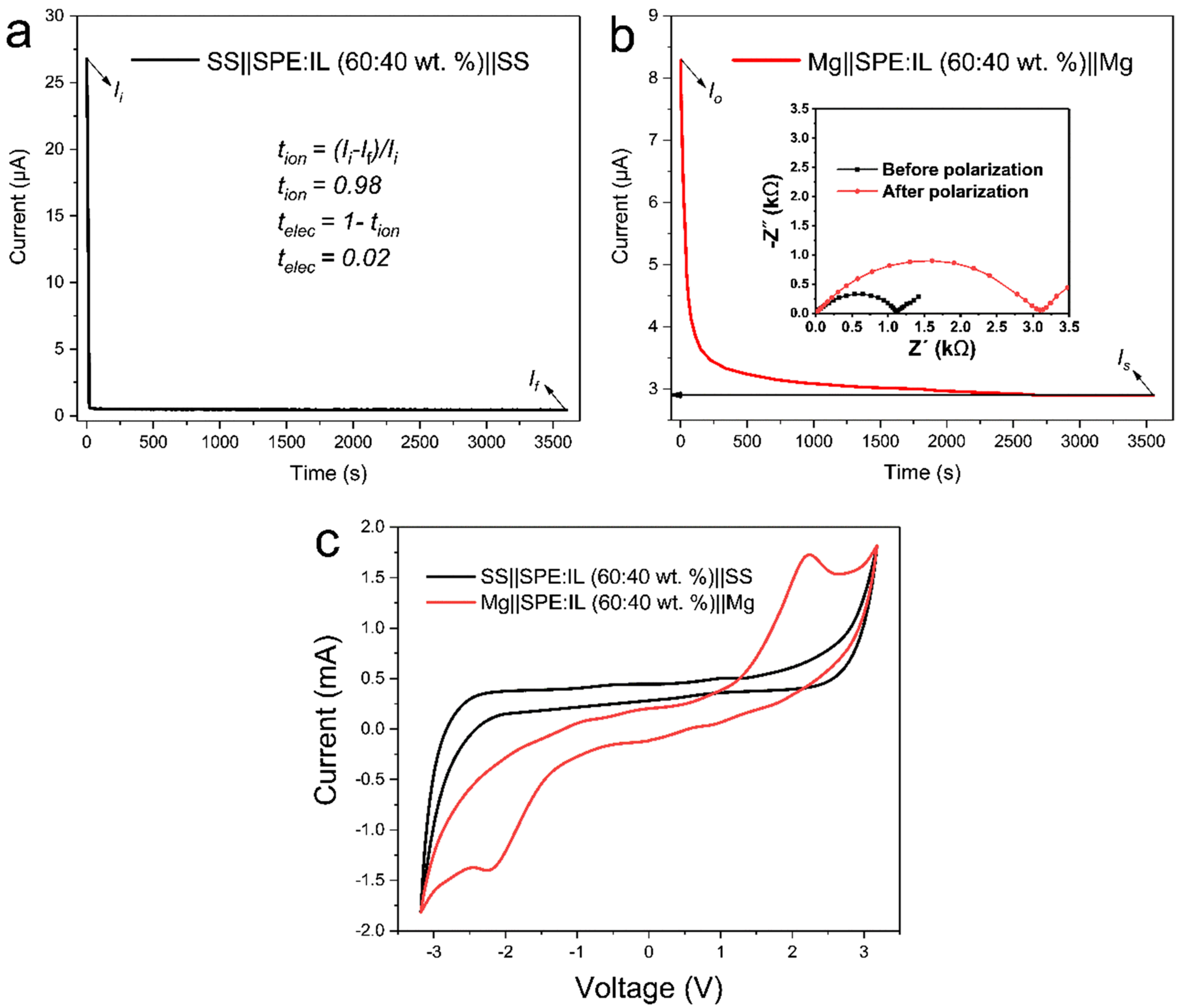


**Fig. 5** **a** Chronoamperometric curve at an applied voltage of 0.75 V and 20 mV on symmetrical cells; SS||SPE:IL (60:40 wt. %)||SS and **b** Mg||SPE:IL (60:40 wt. %)||Mg, respectively. Inset: Impedance curves for symmetrical cell; Mg||SPE:IL (60:40 wt. %)||Mg. **c** Cyclic voltammograms of symmetrical cells; SS||SPE:IL (60:40 wt. %)||SS and Mg||SPE:IL (60:40 wt. %)||Mg. All the electrochemical measurements were carried out at room temperature (30 °C)

## Ionic conductivity

The temperature effect on SPE membranes with different ionic liquid contents is shown in Fig. 4. Conductivity measurements were performed by intercalating SPE membranes between two stainless steel (SS) separators. The dependence of ionic conductivity on temperature was recorded over a range from 30 to 100 °C. An expected behavior of conductivity in SPE:IL (100:0 wt. %), with a certain degree of amorphization, was observed. This behavior can be easily modeled using the VTF equation (Vogel-Tammann-Fulcher) [41]. The addition of ionic liquid [EMIM][$ESO_4$] at 10–20 wt. % in the base membrane produced a discontinuity around the thermal transition zone or from the semi-crystalline to amorphous state in SPE membranes. The discontinuity disappeared when higher amounts of [EMIM][$ESO_4$] (30–40 wt. %) were added. The results confirmed the plasticizing role of [EMIM][$ESO_4$] in SPE membranes, reducing the degree of crystallization, as noted in XRD and DTA studies. Furthermore, this effect has been widely reported in the literature [42]. On the other hand, a quasi-linear behavior of the logarithm of conductivity (log $\sigma$) versus reciprocal temperature ($1/T$), denoting a typical Arrhenius plot, was observed at temperatures below or above the transition zone. This behavior was modeled using the following equation:

$$log\left(\frac{\sigma}{\sigma_o}\right) = -\frac{E_a}{RT} \quad (2)$$

The conduction process activation energy ($E_a$), pre-exponential factor (collision frequency) ($\sigma_o$), universal gas constant ($R$) ($8.6\times10^{-5}$ eV $K^{-1}$), and absolute temperature ($T$) [22] are shown in Table 2. A constant decrease was observed as the ionic liquid concentration increased at room temperature. At 80 °C (a temperature above the semicrystalline-amorphous transition), a large decrease in activation energy was noted, indicating that temperature plays a major role, while the effects of [EMIM][$ESO_4$] addition play a minor role.

## Electrochemical properties and transport number

The total ion transport number ($t_{ion}$) was estimated by chronoamperometry (CA) measurements. In this method the polarization current was controlled as a function of time for the SPE membrane SPE:IL (60:40 wt. %) intercalated between two stainless steel blocking electrodes, employing a symmetrical SS||SPE:IL (60:40 wt. %)||SS cell configuration. A 0.75 V DC was applied across the sample, and the $t_{ion}$ of the SPE membrane was estimated using Wagner's method [43], with the following equation:

$$t_{ion} = \frac{I_i - I_f}{I_i} \quad (3)$$

where $I_i$ (~ 2 6.78 μA) is the initial current and $I_f$ (~ 0.43 μA) is the final steady-state current (Fig. 5a). The $t_{ion}$ value was obtained as 0.98, suggesting the purely ionic nature of the solid polymer electrolyte system.

To determine the transport number ($t_{Mg^{2+}}$), a symmetric cell (Mg||SPE:IL (60:40 wt. %)||Mg) was evaluated using a combination of impedance spectroscopy and polarization studies, as suggested in the literature [44–51], by applying small constant voltage of 20 mV for 1 h. The $t_{Mg^{2+}}$ value was calculated from Eq. (4):

$$t_{Mg^{2+}} = \frac{I_s(\Delta V - R_o I_o)}{I_o(\Delta V - R_s I_s)} \quad (4)$$

where $I_o$ (~ 8.29 μA) and $I_s$ (~ 2.90 μA) are the initial and final steady state currents, and $R_o$ (~ 1123 Ω) and $R_s$ (~ 3116 Ω) are the cell resistance before and after applying the polarization voltage, respectively, as seen in Fig. 5b. Using Eq. (4), the magnesium-ion-transport number is determined to be 0.34. This indicates significant $Mg^{2+}$ ion transport number for the SPE system of this report.

Furthermore, Fig. 5c displays CV tests in symmetrical cells recorded at a scan rate of 5 mV $s^{-1}$. No redox peaks were observed in the SS||SPE:IL (60:40 wt. %)||SS cell, in contrast to the Mg||SPE:IL (60:40 wt. %)||Mg cell, which exhibited reversible redox peaks. This confirms $Mg^{2+}$ ions transfer at the electrolyte/electrode interface [52].

Finally, LSV measurement was employed using SS as working electrode and magnesium disc as counter electrode (Fig. 6), obtaining a high value of ~ 4.2 V, whose electrochemical stability window allowed its application in magnesium ion batteries (see Fig. S5 in the supplementary information for electrochemical performance studies).

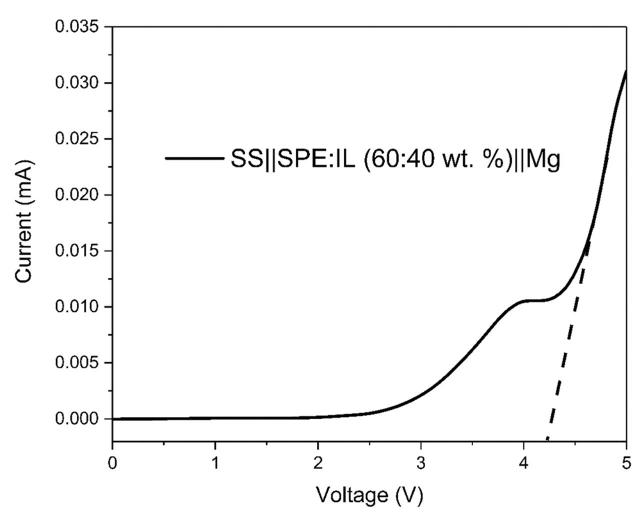


**Fig. 6** LSV test for the cell configuration SS||SPE:IL (60:40 wt. %)||Mg measured at a scan rate of 5 mV $s.^{-1}$

## Conclusions

Solid polymer electrolyte (SPE) membranes based on a PEO/PVDF/$Mg(ClO_4)_2$-[EMIM][$ESO_4$] ternary system were characterized by structural and thermal studies. XRD analysis showed that the SPE membranes had a semicrystalline structure, which promoted good $Mg^{2+}$ ions diffusion. FTIR analysis showed coordination between the $EMIM^+$ cations and $Mg^{2+}$ ions with the oxygens in the PEO polymer, as well as complex formation inside the SPE membrane with a concentration of PEO/PVDF/$Mg(ClO_4)_2$–40 wt. % of [EMIM][$ESO_4$]. The DTA study confirmed that $T_m$ decreased as the IL concentration increased, suggesting an increase in SPE membrane chain flexibility. An ionic conductivity of ~ $5.4 \times 10^{-5}$ S $cm^{-1}$ was observed for the SPE membrane SPE:IL (60:40 wt. %) from the Arrhenius plot, which also showed a total ion transport number of ~ 0.98. These results support a higher contribution of $Mg^{2+}$ ions and a negligible contribution of electrons (~ 0.02) within the SPE system, as well as a high $Mg^{2+}$ ion transport number (~ 0.34). Preliminary studies on rechargeable batteries with a Mg||SPE:IL (60:40 wt. %)||$MoS_2$ configuration showed a discharge capacity of 40 mAh $g^{-1}$.

**Supplementary Information** The online version contains supplementary material available at https://doi.org/10.1007/s11581-023-04968-2.

**Acknowledgements** Authors would like to thank for the laboratory equipment used in this project (Materials Laboratory 2) at División de Estudios de Posgrado. Jesús Guzmán-Torres also thanks to CONACYT for the scholarship awarded to continue the PhD studies.

**Author contribution** Jesús Guzmán-Torres: investigation, validation, software, formal analysis, and writing—original draft. Edgar González-Juárez: electrochemical characterization testing participation. María de la Luz Hernández-Nieto: helped with solid polymer electrolytes preparation. Arián Espinosa-Roa: DFT study participation. Eduardo M. Sánchez: conceptualization, supervision, writing—review and editing, and funding acquisition. All authors read and approved the final manuscript.

**Funding** Authors would like to thank Facultad de Ciencias Químicas, Universidad Autónoma de Nuevo León for financial support.

**Data Availability** The findings of this study are supported by data which can be made available by the corresponding author upon a reasonable institutional request.

## Declarations

**Conflict of interest** The authors declare no competing interests.

## References

1. Bumjun P, Jennifer LS (2020) Review—polymer electrolytes for magnesium batteries: forging away from analogs of lithium polymer electrolytes and towards the rechargeable magnesium metal polymer battery. J Electrochem Soc 167:070545
2. Yang LL, McGhie AR, Farrington GC (1986) Ionic conductivity in complexes of poly(ethylene oxide) and $MgCI_2$. J Electrochem Soc 133:1380
3. Anji RP, Ranveer R (2013) Preparation and characterization of PVA based solid polymer electrolytes for electrochemical cell applications. Chinese J Polym Sci 31:641–648
4. Anji RP, Ranveer K (2011) Conductivity, XRD, and FTIR studies of new $Mg^{2+}$-ion-conducting solid polymer electrolytes: [PEG:$Mg(CH_3COO)_2$]. J Korean Phys Soc 59:114–118
5. Basha SKS, Sundari GS, Kumar KV (2018) Rao MC (2018) Preparation and dielectric properties of PVP-based polymer electrolyte films for solid-state battery application. Polym Bull 75:925–945
6. Aziz AA, Tominaga Y (2018) Magnesium ion-conductive poly(ethylene carbonate) electrolytes. Ionics 24:3475–3481
7. Jeong SK, Jo YK, Jo NJ (2006) Decoupled ion conduction mechanism of poly(vinyl alcohol) based Mg-conducting solid polymer electrolyte. Electrochim Acta 52:1549–1555
8. Viviani M, Meereboer NL, Saraswati NLPA, Loos K, Portale G (2020) Lithium and magnesium polymeric electrolytes prepared using poly(glycidyl ether)-based polymers with short grafted chains. Polym Chem 11:2070
9. Park B, Andersson R, Pate SG, Liu J, O'Brien CP, Hernández G, Mindemark J, Schaefer JL (2021) Ion coordination and transference in magnesium polymer electrolytes based on polyester-co-polycarbonate. Energy Mater Adv 2021: 1–14.
10. Helen PA, Selvin PC, Lakshmi D, Diana MI (2022) Amelioration of ionic conductivity (303K) with the supplement of $MnO_2$ filler in the chitosan biopolymer electrolyte for magnesium batteries. Polym Bull 2022:1–30
11. Rathika R, Suthanthiraraj SA (2016) Ionic interactions and dielectric relaxation of PEO/PVDF-Mg[$(CF_3SO_2)_2N_2$)] blend electrolytes for magnesium ion rechargeable batteries. Macromol Res 24:422–428
12. Anilkumar KM, Jinisha B, Manoj M, Jayalekshmi S (2017) Poly(ethylene oxide) (PEO) - poly(vinyl pyrrolidone) (PVP) blend polymer based solid electrolyte membranes for developing solid state magnesium ion cells. Eur Polym J 89:249–262
13. Bhatt PJ, Pathak N, Mishra K, Kanchan DK, Kumar D (2022) Effect of different cations on ion-transference behavior in polymer gel electrolytes intended for application in flexible electrochemical devices. J Electron Mater 51:1371–1384
14. Singh R, Janakiraman S, Agrawal A, Ghosh S, Venimadhav A, Biswas K (2019) An amorphous poly(vinylidene fluoride-co-hexafluoropropylene) based gel polymer electrolyte for magnesium ion battery. J Electroanal Chem 858:113788
15. Ponraj T, Ramalingam A, Selvasekarapandian S, Srikumar SR, Manjuladevi R (2020) Plasticized solid polymer electrolyte based on triblock copolymer poly(vinylidene chloride-co-acrylonitrile-co-methyl methacrylate) for magnesium ion batteries. Polym Bull 78:35–57
16. Mishra K, Kanchan DK, Gohel K, Sharma P, Kumar D (2022) Urea-assisted ion-transference behavior in magnesium ion conducting solid polymer electrolyte membranes intended for magnesium batteries. Chem Pap 76:827–839
17. Huy VPH, So S, Hur J (2021) Inorganic fillers in composite gel polymer electrolytes for high-performance lithium and non-lithium polymer batteries. J Nanomater 11:614
18. Dhatarwal P, Sengwa RJ (2019) Polymer compositional ratio-dependent morphology, crystallinity, dielectric dispersion, structural dynamics, and electrical conductivity of PVDF/PEO blend films. Macromol Res 27:1009–1023
19. Mohamadi M, Garmabi H, Papila M (2017) Conjugated dual-phase transitions in crystalline/ crystalline blend of poly(vinylidene fluoride)/ poly(ethylene oxide). Polym Bull 74:2117–2135
20. Dhatarwal P, Sengwa RJ (2019) Dielectric relaxation, Li-ion transference, electrochemical, and structural behaviour of PEO/PVDF/$LiClO_4$/$TiO_2$/PC-based plasticized nanocomposite solid polymer electrolyte films. Compos Commun 17:182–191
21. Rathika R, Padmaraj O, Suthanthiraraj SA (2018) Electrical conductivity and dielectric relaxation behaviour of PEO/PVdF-based

solid polymer blend electrolytes for zinc battery applications. Ionics 24:243–255
22. Maheshwaran C, Kanchan DK, Gohel K, Mishra K, Kumar D (2020) Effect of $Mg(CF_3SO_3)_2$ concentration on structural and electrochemical properties of ionic liquid incorporated polymer electrolyte membranes. J Solid State Electrochem 24:655–665
23. Tang X, Muchakayala R, Song S, Zhang Z, Polu AR (2016) A study of structural, electrical, and electrochemical properties of PVdF-HFP gel polymer electrolyte films for magnesium ion battery applications. J Ind Eng Chem 37:67–74
24. Gupta R, Gamare J, Jayachandran K, Gupta SK, Lohithakshan KV, Kamat JV (2015) Electrochemical, thermodynamic and spectroscopic investigations of CeIII in a 1-ethyl-3-methylimidazolium ethyl sulfate (EMIES) ionic liquid. Eur J Inorg Chem 2015:4396–4401
25. Ju Q, Shi Y, Kan J (2013) Performance study of magnesium-polyaniline rechargeable battery in 1-ethyl-3-methylimidazolium ethyl sulfate electrolyte. Synth Met 178:27–33
26. Saroj AL, Singh RK (2012) Thermal, dielectric and conductivity studies on PVA/Ionic liquid [EMIM][$EtSO_4$] based polymer electrolytes. J Phys Chem Solids 73:162–168
27. Polu AR, Rhee HW (2017) Ionic liquid doped PEO-based solid polymer electrolytes for lithium-ion polymer batteries. Int J Hydrog Energy 42:7212–7219
28. Amani AO, Paul N, Muhammad T, Ahmad K, Karim EA, Bassam ET, Malek A (2021) Novel composite membrane based on zirconium phosphate-ionic liquids for high temperature PEM fuel cells. Int J Hydrog Energy 46:6100–6109
29. Daniela MC, Liliana CF, Pedro MM, Clara GA, Carlos MC, Javier R, Senentxu LM (2020) Ionic liquid–polymer composites: a new platform for multifunctional applications. Adv Funct Mater 30:1909736
30. Jesús GT, Dalmy LOG, Lorena LGT, Luis CTG, Salomé MPA, Edgar GJ, Idalia G, Eduardo MS (2023) Magnesium bis(oxalate) borate as a potential electrolyte for rechargeable magnesium ion batteries. J Electron Mater 52:1250–1257
31. Zhang Y, Xiao Q, Lei G, Li Z (2015) An investigation of a novel $MnO_2$ network-Ni/ PVDF double shell/core membrane as an anode for lithium ion batteries. Phys Chem Phys 17:18699–18704
32. Atkore ST, Bondle GM, Kamble VT, Varala R, Adil SF, Hatshan MR, Shaik B (2021) Synthesis, characterization and catalytic evaluation of $ZrCl_4$:$Mg(ClO_4)_2$ for the synthesis of 1,3-diaryl-3-(phenylthio)propan-1-one. J Saudi Chem Soc 25:101359
33. Ponmani S, Prabhu MR (2018) Development and study of solid polymer electrolytes based on PVdFHFP/PVAc: $Mg(ClO_4)_2$ for Mg ion batteries. J Mater Sci: Mater Electron 29:15086–15096
34. Ahmed MB, Nofal MM, Aziz SB, Al-Saeedi SI, Brza MA, Dannoun EMA, Murad AR (2022) The study of ion transference parameters associated with dissociated cation using EIS model in solid polymer electrolytes (SPEs) based on PVA host polymer: XRD, FTIR, and dielectric properties. Arab J Chem 15:104196
35. Reddy MJ, Chu PP (2002) Ion pair formation and its effect in PEO: Mg solid polymer electrolyte system. J Power Sources 109:340–346
36. Nkuna AA, Akpan ED, Obot IB, Verma C, Ebenso EE, Murulana LC (2020) Impact of selected ionic liquids on corrosion protection of mild steel in acidic medium: Experimental and computational studies. J Mol Liq 314:113609
37. Arulsankar A, Kulasekarapandian K, Jeya S, Jayanthi S, Sundaresan B (2013) Investigation of the structural, electrical and morphological properties of $Mg^{2+}$ ion conducting nanocomposite solid polymer electrolytes based on PMMA. Int J Innov Res Technol Sci Eng 2:4883–4890
38. Kiefer J, Fries J, Leipertz A (2007) Experimental vibrational study of imidazolium-based ionic liquids: Raman and infrared spectra of 1-ethyl-3- methylimidazolium Bis(trifluoromethylsulfonyl)imide and 1-ethyl-3-methylimidazolium ethylsulfate. Appl Spectrosc 61:1306–1311
39. Kumar Y, Hashmi SA, Pandey GP (2011) Ionic liquid mediated magnesium ion conduction in poly(ethylene oxide) based polymer electrolyte. Electrochim Acta 56:3864–3873
40. Rathika R, Suthanthiraraj SA (2018) Influence of 1-ethyl-3-methylimidazolium bis (trifluoromethyl sulfonyl) imide plasticization on zinc-ion conducting PEO/PVdF blend gel polymer electrolyte. J Mater Sci: Mater Electron 29:19632–19643
41. Deivanayagam R, Cheng M, Wang M, Vasudevan V, Foroozan T, Medhekar NV, Reza SY (2019) A composite polymer electrolyte for highly cyclable room-temperature solid-state magnesium batteries. ACS Appl Energy Mater 2:7980–7990
42. Correia DM, Fernandes LC, Martins PM, Clara GA, Costa CM, Reguera J, Senentxu LM (2020) Ionic liquid–polymer composites: a new platform for multifunctional applications. Adv Funct Mater 30:1909736
43. Shenbagavalli S, Muthuvinayagam M, Revathy MS, Sasikumar P (2022) Ionic conductivity and dielectric studies on PVP/PEO/$(NH_4)_2Ce(NO_3)_6$ based solid polymer-blend electrolytes. Bull Mater Sci 45:125
44. Evans J, Vincent CA, Bruce PG (1987) Electrochemical measurement of transference numbers in polymer electrolytes. Polymer 28:2324–2328
45. Maheshwaran C, Mishra K, Kanchan DK, Kumar D (2020) $Mg^{2+}$ conducting polymer gel electrolytes: physical and electrochemical investigations. Ionics 26:2969–2980
46. Maheshwaran C, Kanchan DK, Mishra K, Kumar D, Gohel K (2020) Effect of active MgO nano-particles dispersion in small amount within magnesium-ion conducting polymer electrolyte matrix. Nano-Struct Nano-Objects 24:100587
47. Maheshwaran C, Kanchan DK, Mishra K, Kumar D, Gohe K (2020) Flexible magnesium-ion conducting polymer electrolyte membranes: mechanical, structural, thermal, and electrochemical impedance spectroscopic properties. J Mater Sci Mater Electron 31:15013–15027
48. Singh R, Maheshwaran C, Kanchan DK, Mishra K, Singh PK, Kumar D (2021) Ion-transport behavior in tetraethylene glycol dimethyl ether incorporated sodium ion conducting polymer gel electrolyte membranes intended for sodium battery application. J Mol Liq 336:116594
49. Sarangika HNM, Dissanayake MAKL, Senadeera GKR, Rathnayake RRDV, Pitawala HMJC (2017) Polyethylene oxide and ionic liquid-based solid polymer electrolyte for rechargeable magnesium batteries. Ionics 23:2829–2835
50. Guanghai C, Ying B, Yongsheng G, Zhaohua W, Kun Z, Qiao N, Feng W, Huajie X, Chuan W (2019) Inhibition of crystallization of poly(ethylene oxide) by ionic liquid: insight into plasticizing mechanism and application for solid-state sodium ion batteries. ACS Appl Mater Interfaces 11:43252–43260
51. Shishir KS, Himani G, Liton B, Shalu VKS, Alok KT, Yogendra LV, Rajendra KS (2018) Electrochemical characterization of ionic liquid based gel polymer electrolyte for lithium battery application. Ionics 24:1895–1906
52. Buvaneshwari P, Mathavan T, Selvasekarapandian S, Krishna MV, Meera N (2022) Preparation and characterization of biopolymer electrolyte based on gellan gum with magnesium perchlorate for magnesium battery. Ionics 28:3843–3854